Rotating Spin and Giant Splitting: Unoccupied Surface Electronic Structure of Tl/Si(111)

Sebastian D. Stolwijk,* Anke B. Schmidt, and Markus Donath
Physikalisches Institut, Westfälische Wilhelms-Universität Münster, Wilhelm-Klemm-Straße 10, 48149 Münster, Germany

Kazuyuki Sakamoto
Department of Nanomaterials Science, Chiba University, Chiba 263-8522, Japan

Peter Krüger
Institut für Festkörpertheorie, Westfälische Wilhelms-Universität Münster, Wilhelm-Klemm-Straße 10, 48149 Münster, Germany
(Received 26 June 2013; published 23 October 2013)

We present a combined experimental and theoretical study on the unoccupied surface electronic structure of the Tl/Si(111) surface. Spin- and angle-resolved inverse-photoemission measurements with sensitivity to both the in-plane and the out-of-plane polarization direction detect a spin-orbit-split surface state, which is well described by theoretical calculations. We demonstrate that the spin polarization vector rotates from the classical in-plane Rashba polarization direction around $\bar{\Gamma}$ to the direction perpendicular to the surface at the $\bar{K}(\bar{K}')$ points—a direct consequence of the symmetry of the 2D hexagonal system. A giant splitting in energy of about 0.6 eV is observed and attributed to the strong localization of the unoccupied surface state close to the heavy Tl atoms. This leads to completely out-of-plane spin-polarized valleys in the vicinity of the Fermi level. As the valley polarization is oppositely oriented at the $\bar{K}$ and $\bar{K}'$ points, backscattering should be strongly suppressed in this system.

DOI: 10.1103/PhysRevLett.111.176402 PACS numbers: 71.70.Ej, 73.20.At, 79.60.−i

The development of spintronics, i.e., the use of the electron spin as information carrier in electronics, hinges on the generation and manipulation of spin-polarized currents. Here, the Rashba-Bychkov effect [1], i.e., the lifting of the spin degeneracy due to spin-orbit interaction and space inversion asymmetry, opens the way for promising applications [2]. In recent years, it has been demonstrated for several metal surfaces that the Rashba-Bychkov effect leads to a spin-dependent splitting of surface states [3–8]. In some cases, such as Bi/Ag(111) [9] and Bi/Si(111) [10], giant splittings of about 0.2 eV, orders of magnitude larger than those found in semiconductor heterostructures, could be observed—a key factor for an implementation of the surface Rashba-Bychkov effect in spintronics. Briefly, this demands for (i) a metallic surface state with (ii) strong spin-orbit coupling on (iii) a semiconductor surface [11]. As a result, thin films of heavy metals on semiconducting substrates lie in the focus of recent research [10–20].

In this context, the thallium (1×1) overlayer on Si(111) poses an excellent candidate and promotes understanding basic mechanisms of spin-orbit interaction at surfaces. Band structure calculations of the Tl/Si(111)-(1×1) surface reveal an occupied and an unoccupied spin-orbit-split surface state within the fundamental projected bulk-band gap [21]. The symmetry of the 2D honeycomb layered structure in combination with the strong spin-orbit coupling of the adlayer leads to a unique spin pattern in momentum space. Along the $\bar{\Gamma}\,\bar{K}(\bar{\Gamma}\bar{K}')$ direction the polarization vector of the surface states rotates from the polarization direction parallel to the surface and perpendicular to $\mathbf{k}_{\|}$ (classical Rashba polarization direction) to the direction perpendicular to the surface. This is accompanied by a spin-dependent splitting in energy with its maximum at the $\bar{K}(\bar{K}')$ points. Spin- and angle-resolved photoemission experiments demonstrate these characteristic features for the occupied surface state [13]. At $\bar{K}(\bar{K}')$ a splitting in energy of about 0.25 eV is observed. However, here the state is located far below the Fermi level and is therefore hardly relevant for spin-dependent transport phenomena. For the unoccupied electronic structure, theory predicts a surface state with exceptionally large splitting in the vicinity of E_F [21].

In this Letter, we use angle- and spin-resolved inverse-photoemission experiments to unveil the unoccupied spin-orbit-split surface state. We show that, similar to the occupied state, the unoccupied surface state exhibits a rotating polarization vector along $\bar{\Gamma}\,\bar{K}(\bar{\Gamma}\bar{K}')$. Remarkably, at $\bar{K}(\bar{K}')$ the two spin components show an energy splitting of about 0.6 eV. According to our calculation, this exceptionally large splitting is a consequence of the strong localization of the unoccupied surface state close to the Tl atoms. At $\bar{K}(\bar{K}')$, the lower lying surface-state component closely approaches E_F and creates almost completely out-of-plane polarized electron pockets, also referred to as valleys. We will demonstrate that the out-of-plane spin polarization orientation between valleys at $\bar{K}$ and $\bar{K}'$ is reversed. Consequently, backscattering is strongly suppressed [22].

Our Tl/Si(111)-(1×1) films, schematically shown in Figs. 1(a) and 1(b), were prepared by evaporating one monolayer of Tl from a Ta crucible onto a clean n-doped

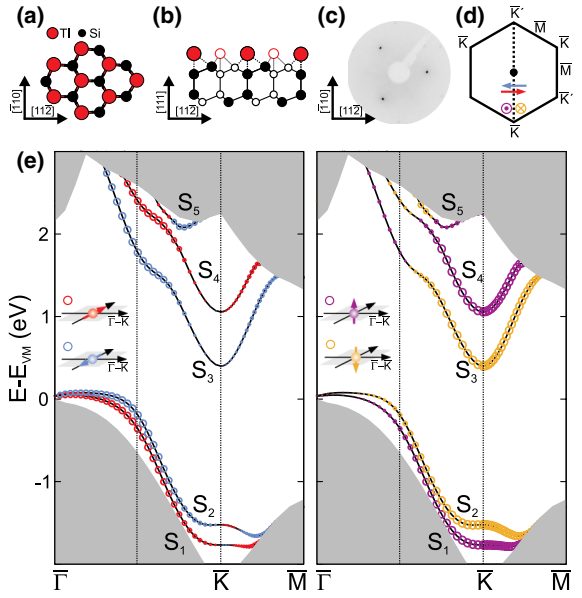

FIG. 1 (color online). (a) Top view and (b) side view of the structural model of the Tl/Si(111)-(1 × 1) surface formed by the adsorption of one monolayer of Tl. (c) Corresponding low-energy electron diffraction image and (d) surface Brillouin zone. (e) Quasiparticle band structures including spin-orbit coupling illustrating the in-plane (left-hand side) and out-of-plane (right-hand side) polarization components. The diameter of the circles is proportional to the spin polarization with a maximum degree of 100%, e.g., for S_4 at $\bar{K}$. The energy scale refers to the valence-band maximum E_{VM}. The gray shaded area illustrates the projected bulk bands.

($10^{15}/\mathrm{cm}^3$) Si(111) substrate at a temperature of 570 K, similar to the recipe given in Ref. [13]. The sharp diffraction pattern and low background intensity of the low-energy electron diffraction image in Fig. 1(c) reflect a well-ordered (1 × 1) structure.

Spin- and angle-resolved inverse-photoemission experiments have been performed using our recently developed homebuilt rotatable spin-polarized electron source [23]. It produces a transversally spin-polarized electron beam with a spin polarization of 29%, whose polarization direction can be chosen freely. This allows measurements of the unoccupied electronic structure with sensitivity to the classical in-plane Rashba and, in addition, for nonnormal electron incidence, to the out-of-plane polarization direction. Spectra have been normalized to 100% spin polarization of the electron beam. The total energy resolution is approximately 350 meV, while the angular resolution of the electron source is ±1.5°. A detailed description of the inverse-photoemission experiment is given in Ref. [24]. Measurements have been conducted at room temperature and were taken along $\bar{\Gamma}\bar{K}$ and $\bar{\Gamma}\bar{K}'$ as indicated by the dotted lines in the surface Brillouin zone in Fig. 1(d).

We start with a discussion of the calculated Tl/Si(111)-(1 × 1) surface electronic structure. The ground-state properties are obtained by using density-functional theory within the local-density approximation. A basis of Gaussian orbitals is employed together with pseudopotentials that include scalar relativistic corrections and spin-orbit coupling [25]. The Tl/Si(111) surface is treated within a supercell approach using slabs with 18 Si substrate layers and a Tl adlayer. Relaxations of the topmost eight layers have been taken into account. Adsorption of Tl atoms in T_4 positions turns out to be energetically most favorable in agreement with former calculations [26]. For determining the quasiparticle band structure, we construct the self-energy operator within the GW approximation [27,28]. Figure 1(e) presents our calculations along $\bar{\Gamma}\bar{K}\bar{M}$. Open circles illustrate the in-plane polarization perpendicular to $\mathbf{k}_\parallel$ (left panel) and the out-of-plane components of the polarization vector (right panel) as defined in Fig. 1(d). No in-plane polarization parallel to $\mathbf{k}_\parallel$ occurs. The size of the circles corresponds to the magnitude of the respective polarization. In accordance with recent band structure calculations [21], one occupied (S_1 and S_2) and one unoccupied (S_3 and S_4) spin-orbit-split surface state is found within the projected bulk-band gap of the silicon substrate. The 2D symmetry of the hexagonal system, belonging to the $p3m1$ space group, leads to $\bar{K}$ and $\bar{K}'$ points with C_3 symmetry. This forces the spin polarization vector to the out-of-plane direction [13,21,29]. Ultimately, the polarization vectors of all four surface-state components rotate from the classical in-plane Rashba direction around $\bar{\Gamma}$ to the out-of-plane direction at $\bar{K}(\bar{K}')$. At this point, an exceptionally large energy splitting of the two unoccupied surface-state components is expected. Our spin- and angle-resolved inverse-photoemission experiments put these predictions to the test.

Figure 2 presents spin- and angle-resolved inverse-photoemission spectra taken at various angles of incidence θ along the $\bar{\Gamma}\bar{K}$ and $\bar{\Gamma}\bar{K}'$ high symmetry lines. Red up- and blue down-pointing triangles represent spin states parallel to the surface and perpendicular to $\mathbf{k}_\parallel$, i.e., the classical in-plane Rashba polarization direction. Purple up- and orange down-pointing triangles denote states with out-of-plane spin polarization, i.e., pointing parallel or antiparallel to the surface normal.

At $\bar{\Gamma}$ ($\theta = 0°$), the two spin states are degenerate. Along $\bar{\Gamma}\bar{K}$, i.e., with increasing angles up to $\theta = 50°$, spin-split bands with in-plane spin polarization emerge. Around $\bar{K}$ ($\theta = 60°$ to $65°$) the in-plane polarization vanishes, as demanded by symmetry considerations. In this region, due to the intrinsic and experimental energy broadening, a splitting of the states is not resolved.

Additional spectra in Fig. 2(b) confirm that the observed spin polarization is in accordance with time-reversal symmetry and the classical Rashba model. Spectra taken at $\theta = 30°$ along $\bar{\Gamma}\bar{K}'$ [lower spectrum in Fig. 2(b)], realized by rotating the azimuth of the sample by 180°, show the same features with similar polarization, whereas measurements at negative angles of incidence [upper spectrum in

Fig. 2(b)], i.e., negative $\mathbf{k}_\parallel$, exhibit a reversed polarization. Note that the sign of the spin polarization is referred to the spin direction of the incoming electron beam.

Figures 2(c) and 2(d) show equivalent measurements with sensitivity to the out-of-plane polarization direction. Importantly, for corresponding angles, the spin-integrated spectra of the in-plane and out-of-plane experiments are almost identical. This verifies the same sample condition and position in $\mathbf{k}$ space. Note that experimental information on the out-of-plane polarization is only accessible for angles θ unequal zero, whereas the effective spin polarization increases with higher θ. Therefore, the spectra at $\theta = 0°$ and 5° have not been normalized to a 100% polarized electron beam. Towards $\bar{K}$, for $\theta > 20°$, several out-of-plane polarized features are detected. Around $\bar{K}'$, the same features appear with opposite polarization [see Fig. 2(d)]. The spin-asymmetry data [$A = (I_\uparrow - I_\downarrow)/(I_\uparrow + I_\downarrow)$] in Fig. 2(e) around $\bar{K}$ and $\bar{K}'$ underline this reversal. The obtained spin-asymmetry values of more than 60% (without background subtraction) strongly indicate almost completely out-of-plane but oppositely polarized states in the vicinity of E_F at $\bar{K}$ and $\bar{K}'$.

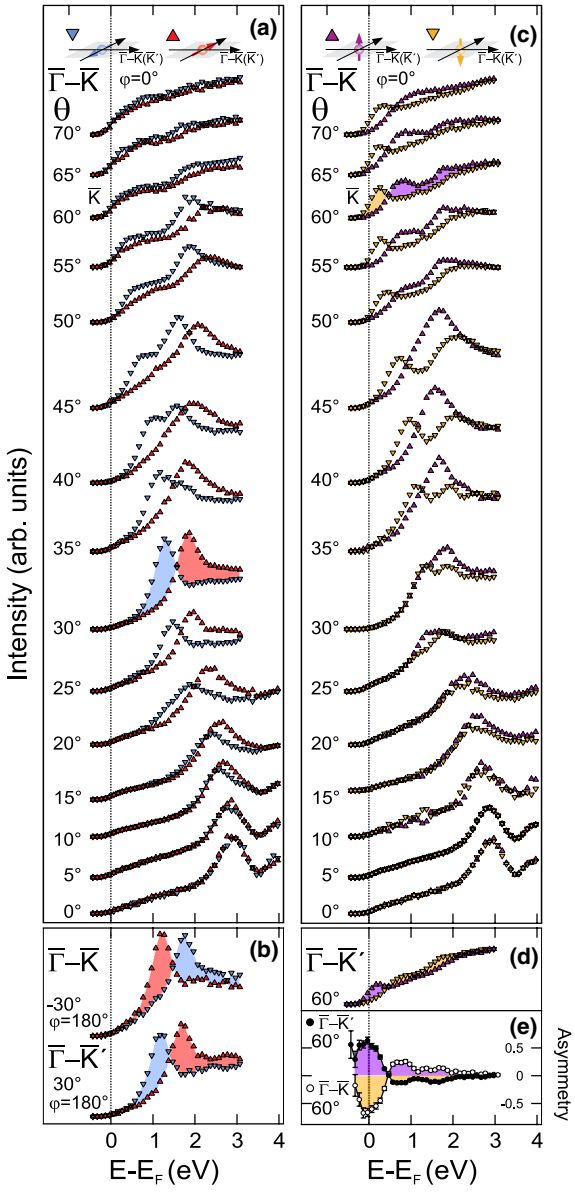

FIG. 2 (color online). Spin- and angle-resolved inverse-photoemission spectra along $\bar{\Gamma}\bar{K}$ and $\bar{\Gamma}\bar{K}'$ sensitive to the (a), (b) in-plane and (c), (d) out-of-plane spin components. θ and ϕ denote the angle of incidence and the sample azimuth, respectively. (e) Out-of-plane spin asymmetry at an angle of incidence $\theta = 60°$ around $\bar{K}$ and $\bar{K}'$.

Spectral features in the in-plane and out-of-plane sensitive inverse-photoemission data are translated into $E(\mathbf{k}_\parallel)$ plots in Figs. 3(a) and 3(b), respectively. The energetic positions of the spectral features were derived by a fitting routine as described in Ref. [30]. For comparison, we show the calculated band dispersion of S_3 and S_4 as solid lines with respect to the Fermi level. E_F lies about 0.25 eV above the highest occupied state S_2 at $\bar{\Gamma}$, independently measured with a photoemission setup in the same apparatus [24], and about 0.2 eV below the lowest unoccupied state S_3 at $\bar{K}$. ΔE between S_2 at $\bar{\Gamma}$ and S_3 at $\bar{K}$ amounts to 0.45 eV, which agrees well with 0.36 eV found in our calculation.

A total of four states S_3 to S_6 are measured. S_5 and S_6 are interpreted as surface-resonant states and will not be discussed further. Most prominent are the two strongly downward dispersing features S_3 and S_4 with minimum energy at $\bar{K}$ ($\mathbf{k}_\parallel \approx 1.1$ Å^{-1}). In comparison with our band structure calculations, S_3 and S_4 are easily identified as the two components of the unoccupied spin-orbit-split surface

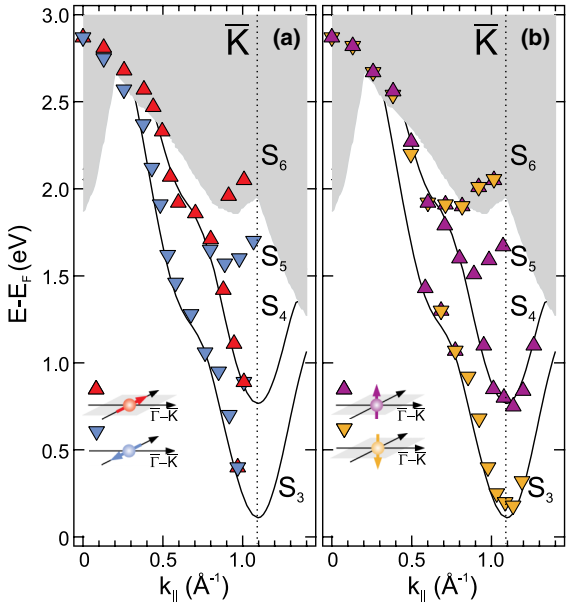

FIG. 3 (color online). E vs $\mathbf{k}_\parallel$ plot derived from spectra taken along $\bar{\Gamma}\bar{K}$ with sensitivity to (a) the in-plane and (b) the out-of-plane polarization. Solid lines show the calculated surface-state bands.

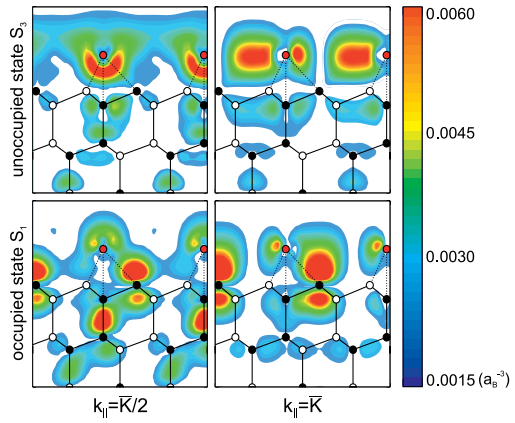

FIG. 4 (color online). Charge distribution plots of the occupied and unoccupied surface-state component S_1 and S_3 at two points in $\mathbf{k}$ space $\bar{K}/2$ and $\bar{K}$.

state. In the following we will discuss (i) the spin splitting and (ii) the polarization of the unoccupied surface state.

(i) At $\bar{K}$, the lower lying surface-state component S_3 closely approaches E_F. Here, S_3 and S_4 exhibit a giant spin-dependent splitting in energy of about 0.6 eV. This splitting is almost two-thirds of the atomic spin-orbit splitting of a thallium p state [$\Delta E = (2l+1)\lambda \approx 0.9$ for $l = 1$, $\lambda \approx 0.3$ eV], larger by more than a factor of 2 than observed in the occupied surface-state components S_1 and S_2 [13]. Charge distribution plots in Fig. 4 of the occupied and unoccupied surface-state components S_1 and S_3 provide an explanation. At $\bar{K}$ and $\bar{K}'$, the unoccupied state is mainly localized at the Tl atoms, whereas the occupied surface state is localized at the Si atoms. Charge distribution plots without considering spin-orbit interaction indicate similar results [26]. The nature of the giant splitting is, therefore, assigned to the proximity of the unoccupied surface state to the heavy nuclei [31].

(ii) Figures 2 and 3 give an overall picture of the polarization of the unoccupied surface-state components. Around the $\bar{\Gamma}$ point, S_3 and S_4 exhibit only in-plane polarization. This in-plane polarization is retained up to $k_{\|} \approx 0.85$ Å^{-1} ($\theta = 45°$). For higher $k_{\|}$ values it decreases and ultimately vanishes at $\bar{K}$. Out-of-plane polarization first appears at $k_{\|} \approx 0.6$ Å^{-1} ($\theta = 25°$). Here, S_3 is up-polarized. At $k_{\|} \approx 0.7$ Å^{-1} S_3 exhibits no out-of-plane polarization. For increasing $k_{\|}$ values S_3 is down-polarized. At the $\bar{K}$ point S_3 and S_4 are almost completely out-of-plane polarized. In total, a rotation of the polarization vector is observed. This coincides with the theoretical findings.

In principle, the rotation of the polarization vector can already be understood by applying a simple tight binding model, taking into account the Si dangling bond and the Tl p_x, p_y, p_z orbitals. Interaction of the Tl p_z orbital with the Si substrate induces a potential gradient along the surface normal, resulting in a classical in-plane Rashba polarization. Interaction of the p_x, p_y orbitals with the substrate induces an in-plane inversion asymmetry resulting in an out-of-plane polarization. As the surface states S_3 and S_4 are predominantly of p_z character around $\bar{\Gamma}$ and purely of p_x, p_y character at $\bar{K}$, a transition from in-plane to out-of-plane polarization takes place. At $\bar{K}$ these states are completely polarized since spin-orbit coupling does not intermix spin-up with spin-down components of p_x and p_y orbitals. The charge distribution plots in Fig. 4 of the unoccupied surface-state component S_3 at two points in $\mathbf{k}$ space comply with this model. Halfway between $\bar{\Gamma}$ and $\bar{K}$ (marked by vertical lines in Fig. 1) the charge distribution is predominately asymmetric along the surface normal, which is related to an in-plane spin polarization. On the other hand, at $\bar{K}$ in-plane asymmetry is dominant, which relates to an out-of-plane polarization.

In conclusion, our experimental study of the unoccupied electronic structure of Tl/Si(111) with sensitivity to the in-plane and out-of-plane polarization components demonstrates the unique properties of the unoccupied surface state. We have unambiguously shown that the polarization vector of the unoccupied Tl/Si(111) surface state rotates from the classical in-plane Rashba direction to the direction perpendicular to the surface. Furthermore, at $\bar{K}$ the unoccupied surface state shows a giant splitting in energy of about 0.6 eV. The extraordinary large splitting is traced back to the strong localization close to the Tl atoms. As a result, almost completely out-of-plane polarized valleys are formed in the vicinity of E_F at $\bar{K}$ and $\bar{K}'$. This out-of-plane polarization direction is opposite at $\bar{K}$ and $\bar{K}'$. All findings are in excellent agreement with theory. We note a resemblance to MoS_2, a system which has attracted immense attention in the field of valleytronics [32–35]. In both systems, the valleys at $\bar{K}$ and $\bar{K}'$ carry opposite Berry curvature. This allows for transverse currents where electrons with antipodal spin flow to opposite sides of the sample when an electrical field is applied in the surface plane. Further spin- and angle-resolved photoemission experiments on doped Tl/Si(111) surfaces reveal a shift of the unoccupied surface state. The lower lying valley becomes metallic and creates a peculiar Fermi surface, where backscattering is strongly suppressed [22].

Financial support by the Deutsche Forschungsgemeinschaft is gratefully acknowledged. K. S. was supported by the Grant-in-Aid for Scientific Research (A) No. 20244045 and (B) No. 25287070.

*sebastian.stolwijk@wwu.de

[1] Y. A. Bychkov and E. I. Rashba, JETP Lett. **39**, 78 (1984).
[2] S. Datta and B. Das, Appl. Phys. Lett. **56**, 665 (1990).
[3] S. LaShell, B. A. McDougall, and E. Jensen, Phys. Rev. Lett. **77**, 3419 (1996).
[4] M. Hochstrasser, J. G. Tobin, E. Rotenberg, and S. D. Kevan, Phys. Rev. Lett. **89**, 216802 (2002).

[5] M. Hoesch, M. Muntwiler, V. N. Petrov, M. Hengsberger, L. Patthey, M. Shi, M. Falub, T. Greber, and J. Osterwalder, Phys. Rev. B **69**, 241401 (2004).
[6] Y. M. Koroteev, G. Bihlmayer, J. E. Gayone, E. V. Chulkov, S. Blügel, P. M. Echenique, and P. Hofmann, Phys. Rev. Lett. **93**, 046403 (2004).
[7] K. Sugawara, T. Sato, S. Souma, T. Takahashi, M. Arai, and T. Sasaki, Phys. Rev. Lett. **96**, 046411 (2006).
[8] A. Tamai, W. Meevasana, P. D. C. King, C. W. Nicholson, A. de la Torre, E. Rozbicki, and F. Baumberger, Phys. Rev. B **87**, 075113 (2013).
[9] C. R. Ast, J. Henk, A. Ernst, L. Moreschini, M. C. Falub, D. Pacilé, P. Bruno, K. Kern, and M. Grioni, Phys. Rev. Lett. **98**, 186807 (2007).
[10] I. Gierz, T. Suzuki, E. Frantzeskakis, S. Pons, S. Ostanin, A. Ernst, J. Henk, M. Grioni, K. Kern, and C. R. Ast, Phys. Rev. Lett. **103**, 046803 (2009).
[11] K. Yaji, Y. Ohtsubo, S. Hatta, H. Okuyama, K. Miyamoto, T. Okuda, A. Kimura, H. Namatame, M. Taniguchi, and T. Aruga, Nat. Commun. **1**, 1 (2010).
[12] I. Barke, F. Zheng, T. K. Rügheimer, and F. J. Himpsel, Phys. Rev. Lett. **97**, 226405 (2006).
[13] K. Sakamoto, T. Oda, A. Kimura, K. Miyamoto, M. Tsujikawa, A. Imai, N. Ueno, H. Namatame, M. Taniguchi, P. E. J. Eriksson, and R. I. G. Uhrberg, Phys. Rev. Lett. **102**, 096805 (2009).
[14] S. Hatta, T. Aruga, Y. Ohtsubo, and H. Okuyama, Phys. Rev. B **80**, 113309 (2009).
[15] S. Mathias, A. Ruffing, F. Deicke, M. Wiesenmayer, I. Sakar, G. Bihlmayer, E. V. Chulkov, Y. M. Koroteev, P. M. Echenique, M. Bauer, and M. Aeschlimann, Phys. Rev. Lett. **104**, 066802 (2010).
[16] T. Okuda, K. Miyamaoto, Y. Takeichi, H. Miyahara, M. Ogawa, A. Harasawa, A. Kimura, I. Matsuda, A. Kakizaki, T. Shishidou, and T. Oguchi, Phys. Rev. B **82**, 161410 (2010).
[17] P. Höpfner, J. Schäfer, A. Fleszar, S. Meyer, C. Blumenstein, T. Schramm, M. Heßmann, X. Cui, L. Patthey, W. Hanke, and R. Claessen, Phys. Rev. B **83**, 235435 (2011).
[18] A. Takayama, T. Sato, S. Souma, and T. Takahashi, Phys. Rev. Lett. **106**, 166401 (2011).
[19] P. Kocán, P. Sobotík, and I. Ošt'ádal, Phys. Rev. B **84**, 233304 (2011).
[20] Y. Ohtsubo, S. Hatta, H. Okuyama, and T. Aruga, J. Phys. Condens. Matter **24**, 092001 (2012).
[21] J. Ibañez-Azpiroz, A. Eiguren, and A. Bergara, Phys. Rev. B **84**, 125435 (2011).
[22] K. Sakamoto, T.-H. Kim, T. Kuzumaki, B. Müller, Y. Yamamoto, M. Minoru Ohtaka, J. Osiecki, K. Miyamoto, Y. Takeichi, A. Harasawa, S. D. Stolwijk, A. B. Schmidt, J. Fujii, R. I. G. Uhrberg, M. Donath, H. W. Yeom, and T. Oda, Nat. Commun. **4**, 2073 (2013).
[23] S. D. Stolwijk, H. Wortelen, A. B. Schmidt, and M. Donath (to be published).
[24] M. Budke, T. Allmers, M. Donath, and G. Rangelov, Rev. Sci. Instrum. **78**, 113909 (2007).
[25] B. Stärk, P. Krüger, and J. Pollmann, Phys. Rev. B **84**, 195316 (2011).
[26] S. S. Lee, H. J. Song, K. D. Kim, J. W. Chung, K. Kong, D. Ahn, H. Yi, B. D. Yu, and H. Tochihara, Phys. Rev. B **66**, 233312 (2002).
[27] M. S. Hybertsen and S. G. Louie, Phys. Rev. B **37**, 2733 (1988).
[28] C. Sommer, P. Krüger, and J. Pollmann, Phys. Rev. B **85**, 165119 (2012).
[29] T. Oguchi and T. Shishidou, J. Phys. Condens. Matter **21**, 092001 (2009).
[30] S. D. Stolwijk, A. B. Schmidt, and M. Donath, Phys. Rev. B **82**, 201412 (2010).
[31] M. Nagano, A. Kodama, T. Shishidou, and T. Oguchi, J. Phys. Condens. Matter **21**, 064239 (2009).
[32] D. Xiao, G.-B. Liu, W. Feng, X. Xu, and W. Yao, Phys. Rev. Lett. **108**, 196802 (2012).
[33] K. F. Mak, K. He, J. Shan, and T. F. Heinz, Nat. Nanotechnol. **7**, 494 (2012).
[34] H. Zeng, J. Dai, W. Yao, D. Xiao, and X. Cui, Nat. Nanotechnol. **7**, 490 (2012).
[35] W. Feng, Y. Yao, W. Zhu, J. Zhou, W. Yao, and D. Xiao, Phys. Rev. B **86**, 165108 (2012).